



Microwave swing regeneration of aqueous monoethanolamine for post-combustion CO₂ capture



Stephen J. McGurk, Claudia F. Martín¹, Stefano Brandani, Martin B. Sweatman*, Xianfeng Fan*

Institute for Materials and Processes, School of Engineering, University of Edinburgh, Mayfield Road, Edinburgh EH9 3JL, UK

HIGHLIGHTS

- Microwaves can regenerate CO₂ rich MEA solution quickly and at 70–90 °C.
- Microwave regeneration can reduce energy penalty, corrosion, amine degradation.
- Microwaves regeneration presents a special 'non-thermal' effect.
- Fast regeneration can reduce the size of a capture process.

ARTICLE INFO

Article history:

Received 22 September 2016

Received in revised form 16 January 2017

Accepted 6 February 2017

Keywords:

CO₂ capture
Amine
Energy
Microwave
Absorption kinetics
Absorption isotherm

ABSTRACT

Post-combustion carbon capture is a key component of the fight against global warming and climate change. Amine stripping is currently the leading post-combustion technology, and indeed is employed at the World's first and only commercial scale carbon capture project applied to a power plant, at Boundary Dam, Canada. Normally, regeneration of the spent amine solution is achieved by stripping with hot pressurized steam, at around 120–140 °C and 1–2 bar. However, production of these conditions is costly and leads to significant degradation of the amine. Moreover, the size of equipment, and hence capital costs, are also high due to the regeneration timescales involved. Here, we present proof-of-concept laboratory scale experiments to demonstrate the feasibility of regenerating the spent amine solution with microwave irradiation. We show that microwaves can regenerate spent aqueous monoethanolamine solutions quickly and at low temperatures (70–90 °C), potentially reducing overall process costs. By comparing microwave regeneration with conventional thermal regeneration we suggest that, in addition to the usual benefits of microwave heating, microwaves present a special 'non-thermal' effect.

© 2017 The Authors. Published by Elsevier Ltd. This is an open access article under the CC BY license (<http://creativecommons.org/licenses/by/4.0/>).

1. Introduction

Anthropogenic greenhouse gas emissions are the leading cause of global warming, with the primary contributor, CO₂, surpassing a record 400 ppmv atmospheric concentration in November 2015 [1]. Fossil fuel usage accounts for around 91% of total CO₂ emissions from human sources [2], however their continued use remains vital to meet current energy demands [3,4]. Post-combustion CO₂ capture (PC-CC) is widely considered as one of the most effective near-term mitigation strategies for combating CO₂ emissions [5]. The most matured PC-CC technology is amine scrubbing [6], which is a continuous cyclic process of CO₂

absorption and desorption typically performed in two packed columns [7]. Flue gas containing CO₂ passes through the bottom of an absorber column and contacts the CO₂-lean absorbent between 40 °C and 60 °C at atmospheric pressure [8]. The CO₂-rich solvent flows to the stripper column for thermal regeneration using hot steam between 120 °C and 140 °C and 1–2 bar to produce a purified (>99%) outlet CO₂ stream [9,10]. The CO₂-lean solution exits the bottom of the stripper and recirculates to the absorber column via a crossed heat exchanger ready for the next cycle [8]. The industry benchmark amine is monoethanolamine (MEA), typically employed as a 30 weight percent (wt%) solution in water [4]. CO₂ reacts with the solvated MEA to form a stable and soluble carbamate salt, as shown in Reaction 1, which may proceed to higher loading through hydration reactions. Application of heat reverts back to the original amine solution and recovers the free CO₂ [11–14].

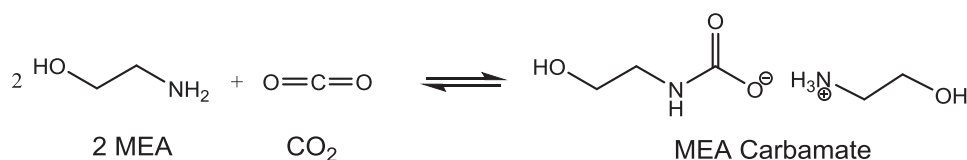
* Corresponding authors.

E-mail addresses: Martin.Sweatman@ed.ac.uk (M.B. Sweatman), X.Fan@ed.ac.uk (X. Fan).

¹ Present address: School of Engineering, University of Aberdeen, King's College, Aberdeen AB24 3UE, UK.

Nomenclature

$\varepsilon^*(\omega)$	frequency-dependent complex permittivity	E	electric field strength (V/m)
$\varepsilon'(\omega)$	real part of complex permittivity	V	dielectric volume (m ³)
$\varepsilon''(\omega)$	imaginary part of complex permittivity	ε_0	permittivity of free-space (8.854×10^{-12} F/m)
ω	angular frequency (Hz)		
P_{abs}	absorbed microwave power (W)		



Reaction 1 – The reaction of MEA with CO₂ to form a carbamate.

Amine scrubbing is a proven, if expensive, technology. The dominant process costs arise from the large equipment size, the heat required during regeneration and thermal degradation of the solvent at the high processing temperatures [4,15]. Solutions to these problems have tended to focus on development of better solvents and optimization of the process configuration [16–19]. Here, we outline proof-of-concept laboratory scale experiments to test the feasibility of microwave swing regeneration (MSR) as an alternative approach to the conventional thermal recovery of CO₂ from a rich MEA solution. This is motivated by recent literature highlighting microwave heating as an effective means of regenerating solid adsorbents for CO₂ capture and storage [20–23]. Microwave, or dielectric, heating refers to the direct heating of a sample through interaction with electromagnetic radiation. As such, microwaves offer instantaneous and volumetric heating without [24] heat transfer restrictions associated with conventional conductive or convective heating [25]. For polar solvents, such as water or MEA, microwave heating primarily takes place via reorientation of molecular dipoles in the presence of the rapidly oscillating electric field [24,25]. A phase lag between the molecular motion and the electric field causes friction between neighbouring molecules, which ultimately leads to dissipation of the electromagnetic energy into heat [26,27]. Other important loss mechanisms occur through ion conduction in ionic solutions and Maxwell-Wagner polarization, resulting from interfacial phenomena, in inhomogeneous media [27].

The susceptibility of a substance to microwave heating is governed by its frequency-dependent complex permittivity [24]:

$$\varepsilon^*(\omega) = \varepsilon'(\omega) - i\varepsilon''(\omega) \quad (1)$$

where the real part, $\varepsilon'(\omega)$, is a measure of the polarizability of the dielectric by an external field and the imaginary part, $\varepsilon''(\omega)$ is the dielectric loss factor, which represents the ability to convert absorbed microwave energy into heat [24]. The average power per unit volume absorbed by a sample during microwave heating, P_{abs} (W), is proportional to its dielectric response and also affected by microwave field properties, specifically the angular frequency, ω (Hz), and the average electric field strength, E (V/m), which is determined by the inlet power and local electric field distribution [28]:

$$P_{abs} = \omega \varepsilon_0 \varepsilon''(\omega) |E|^2 V \quad (2)$$

where ε_0 is the permittivity of free-space (8.854×10^{-12} F/m) and V is the sample volume (m³).

Microwave technology has long been acknowledged as an effective means to intensify chemical processes [24]. Applications have traditionally centred around microwave-assisted organic synthesis and solid adsorption-desorption systems for desiccant dehydration, volatile organic compound (VOC) recovery, air separation and water purification [24,25,27]. Many studies have reported more efficient chemical productivity and economic performance with MSR compared to conventional regeneration techniques, owing to the direct and rapid nature of microwave heating. Cherbanski et al. compared the desorption kinetics of MSR to conventional temperature swing regeneration (TSR) for acetone and toluene removal from zeolite 13X molecular sieves [29]. They revealed more efficient desorption with MSR due to the direct and instantaneous heating of the adsorbent by microwave radiation, becoming more pronounced for the more polar adsorbate [29]. Hashisho and co-workers developed an MSR system for the adsorptive separation of organic vapours and binary gas mixtures, including CO₂/CH₄, with activated carbons and titanosilicate Na-ETS-10. Microwave desorption was found to be up to 40 times faster than conductive thermal heating and more energy efficient over multiple regeneration cycles [30–36]. Ania et al. illustrated the effects of microwave and conventional thermal regeneration on the structure and adsorptive capacity of activated carbons. An inverted temperature gradient during microwave heating encouraged diffusion of the desorbing molecules from the core of the carbon bed towards the surface leading to shorter regeneration times [37]. Polaert and co-workers have made extensive use of MSR for a broad range of solid adsorbents for water and VOC recovery [38,39]. The absorbed microwave power and dielectric properties were concluded to be the most important parameters in ensuring a favourable economic performance. Optimization of the experimental design lead to important energy savings compared to conventional TSR [38,39]. Turner et al. investigated the influence of microwave radiation on sorption and competitive sorption of polar and non-polar adsorbates in high-silica zeolites [40]. The microwaves permitted greater sorption selectivity, and also generated interesting surface temperature effects. Due to the extremely low dielectric response of silica, the bulk zeolite couples negligibly to the microwaves, however the surface silanol (hydroxyl) groups possess significant dielectric loss parameters and couple strongly

to the microwaves. It was proposed that the surface silanol groups selectively absorb microwave energy and heat the zeolite surface. This lowers the overall energy demand of the desorption process, as energy is targeted at the adsorbed phase without directly heating the bulk. Accordingly, their measurements indicated that less than half the energy was required for microwave regeneration compared to conventional approaches, such as resistive heating or steam stripping [40]. Similarly, Vallee and Conner proposed a localized surface temperature effect for sorption of VOCs on oxides, such as high silica zeolites [41]. These additional contributions unique to microwave heating are so-called “non-thermal” effects, which may influence a chemical or physical process without significantly altering the effective temperature of the whole system [24]. Antonio and Deam suggested that such microwave-specific effects are a consequence of enhanced diffusion properties following dipolar realignment under the applied electric field [42].

To date there have been only a few studies of microwave regeneration exclusively aimed at CO₂ capture and recovery. Conclusions of these studies centre around the chemical selectivity of the microwaves, accelerated desorption rates, high cyclic stability and potential energy savings compared to conventional thermal heating. Webley and Zhang employed microwave-assisted vacuum regeneration of zeolite 13X for CO₂ recovery from wet flue gas [20]. The authors commented on the selective ability of microwaves to target different chemical species and on the manifestation of thermal and non-thermal effects [20]. Chronopoulos et al. compared the CO₂ desorption rates of microporous activated carbon using MSR in a multimode microwave oven to conventional TSR [21]. The results displayed an increased CO₂ desorption rate for MSR, four times faster than for latter method. Yang et al. applied microwave regeneration to perfluorinated silica-stabilized dry alkanolamines for CO₂ capture [22]. They reported exceptional sorbent recyclability as well as a ten-fold decrease in energy requirements. Most recently, Nigar and co-workers investigated CO₂ adsorption and desorption from amine-functionalized mesoporous silica using microwave heating [23]. The CO₂ load, dielectric response and heating rates were found to increase proportionally with amine functionalization. Adsorbent regeneration was up to four times faster when compared to conventional heating, exhibiting high stability over multiple cycles [23]. However, unlike amine stripping, none of these capture technologies is used commercially for carbon capture, and therefore they are often called ‘second generation’. Here, we focus instead on ‘first generation’ capture technology, i.e. amine scrubbing, which is in commercial use.

2. Materials and methods

2.1. Experimental configuration

We employ a laboratory-scale bubble column reactor with 30 wt% aqueous MEA solution within a single mode microwave applicator at 2.45 GHz. The basis of the microwave regeneration experiment is outlined in Fig. 1 and consists of a WR340 rectangular waveguide (86.36 mm × 43.18 mm) connected to a 2450 MHz magnetron (GAE Inc., GA4001, maximum power 1.2 kW, peak voltage 4.5 kV) controlled by an Alter SM445 switching power supply. The waveguide incorporates a three-port circulator (GAE Inc., GA1105) with a cross dummy load, a dual-directional coupler (GAE Inc., GA310x, coupling factor 60 dB, directivity 23 dB) with GA3301 coupler power interfaces, a three-stub tuner (GAE Inc., GA1005), universal waveguide applicator (GAE Inc., GA600x), and a sliding short circuit (Sairem). The microwaves are generated by the magnetron with an adjustable input power setting and are then directed through the circulator and down the longitudinal axis of the waveguide.

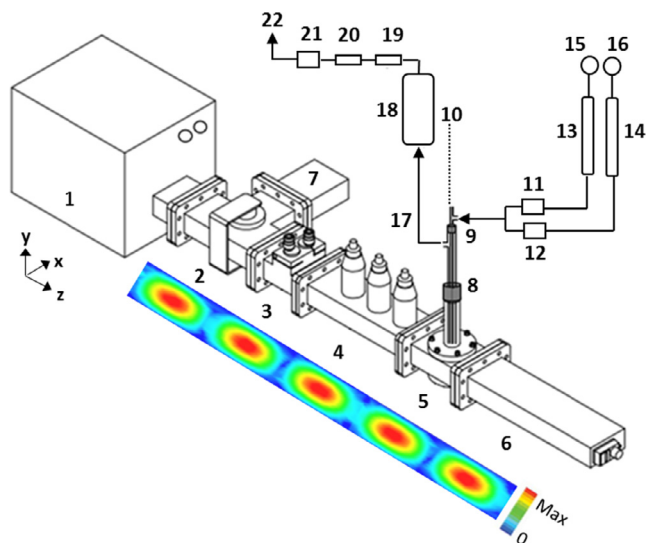


Fig. 1. The configuration of the microwave regeneration experiment. (1) Magnetron, (2) circulator, (3) dual-directional coupler and interfaces, (4) three-stub tuner, (5) universal waveguide applicator, (6) sliding short circuit, (7) water dummy load, (8) quartz bubbler, (9) gas inlet to bubbler, (10) fibre-optic temperature sensor and signal conditioner, (11) CO₂ mass flow controller, (12) N₂ mass flow controller, (13) zeolite/silica drying column for CO₂ gas line, (14) zeolite/silica drying column for N₂ gas line, (15) CO₂ gas cylinder and regulator, (16) N₂ gas cylinder and regulator, (17) gas outlet from bubbler, (18) water condenser, (19) humidity meter, (20) CO₂ sensor, (21) mass flow meter, (22) gas exit. Numbers 2 to 6 make up the waveguide. Numbers 1, 3, 10, 11, 12, 19, 20 and 21 are connected to an experimental computer through a National Instruments DAQ interface and LabView routine for data acquisition and control. A representation of the propagating electric field magnitude along the waveguide is also shown. This figure was adapted with permission from Gerling Applied Electronics, Inc.

The WR340 waveguide propagates the microwave electric field in the dominant TE₁₀ mode (guide wavelength = 17.35 cm), as portrayed in Fig. 1, meaning that the electric field is uniform and transverse to the direction of propagation. After passing through the dual-directional coupler and three-stub tuner, the input wave travels through the waveguide applicator and interacts with the loaded sample. The wave then undergoes reflection at normal incidence from the short circuit and is directed back through the sample region along the reverse direction of the input wave, where finally the power is dumped into the dummy (water) load. A superposition of the forward and reflected waves creates a standing wave within the sample interaction region. The three-stub tuner and sliding short circuit are manually adjusted before each set of experiments to minimize impedance mismatch of the sample load and shift the peak of the electric field intensity to the sample. This ensures maximum power transfer efficiency during the microwave heating. The dual-directional coupler monitors the forward and reverse power flow across the waveguide.

A solution of 30 wt% MEA (Sigma Aldrich, >99% purity) in distilled water was contained in a cylindrical quartz bubbler reactor (17 mm × 135 mm) and placed in the waveguide applicator. Quartz was chosen due to its transparency in the microwave region ($\epsilon'' < 0.001$) [28] and the bubbler was sealed using PTFE collars. The temperature of the liquid was monitored using a fibre-optic temperature sensor (Opsens OTG-MPK8) and signal conditioner, suited for use with amine solutions and microwaves. Research grade gases (Linde Group, >99.99% purity) were fed into the quartz bubbler via two mass flow controllers (Brooks Instruments GF-Series, 0–400 mL/min N₂, 0–100 mL/min CO₂). The outlet gas line from the bubbler was cooled and connected to a cold trap to minimize evaporation losses. The outlet gas stream from the bubbler passed successively through a humidity meter and non-dispersive infrared (NDIR) CO₂ sensor (COZIR-W-100) followed by a mass flow meter

(Brooks Instruments SLA5860, 0–500 mL/min) before exiting through an exhaust line. All experiments were performed at a total pressure of 1 bar. The gas lines were purged with N_2 before and between experimental runs.

2.2. Experimental procedure

Four sets of experiments were performed: heating and cooling profiles, comparison of conventional and microwave regeneration, CO_2 absorption isotherms and multiple microwave regeneration cycles. For the heating and cooling profiles, 5 mL samples were separately heated in a water bath and the microwave applicator at an input power of 100 W between room temperature and 70 °C with 100 mL/min N_2 bubbling through. The solution was then left to cool by removing the heat source. The samples used were water, 30 wt% MEA and 30 wt% MEA previously loaded with CO_2 during a 20 min absorption step.

For the regeneration experiments, during the absorption step a binary gas feed of 20% CO_2 and 80% N_2 was bubbled through 5 mL MEA solution at 100 mL/min for 20 min at ambient temperature. A blank absorption run was performed with an empty reactor to allow the absorbed quantity of CO_2 to be calculated. For the desorption step, the CO_2 was stopped and the input N_2 flow rate set to 100 mL/min. The CO_2 -rich solution was heated to the desired regeneration temperature (70 °C or 90 °C) and held there for 10 min, followed by 10 min with no heating. The microwave heating was performed at an initial input power of 100 W to reach the desired temperature and then the power manually adjusted at around 40 W for 70 °C and 60 W for 90 °C to maintain a constant temperature. Conventional heating experiments were performed in a water bath at the regeneration temperature. The outlet CO_2 flow rates were determined by taking the CO_2 sensor reading as a percentage of the total mass flow meter reading. The volume of CO_2 absorbed was calculated by integrating the difference between the blank and sample CO_2 outlet flow rates. The amount of CO_2 released by the desorption step was determined by direct integration of the outlet CO_2 flow rate. The steady-state CO_2 loadings could then be ascertained by difference of the absorbed and desorbed quantities.

For the isotherm experiments, the quartz bubbler containing 7 mL of 30 wt% MEA solution was continually heated at 65 °C either in the microwave applicator or in a water bath. Heating continued well past the point at which a steady temperature was achieved (with heat dissipated to the surroundings through the un-lagged quartz vessel in the case of microwave heating). A gas feed of 20% CO_2 and 80% N_2 , to provide an inlet CO_2 partial pressure 20 kPa, was bubbled through the solution at 50 mL/min for up to 4 h until a material steady-state was achieved, i.e. the liquid became saturated at the given gas partial pressures. The CO_2 partial pressure was then increased to 29 kPa and the system left for steady-state to re-establish. Due to the continuous bubbling the temperature distribution within the bubbler is expected to be very even. A blank run was also performed without any MEA solution to determine the amount of CO_2 absorbed. Equilibrium CO_2 loadings were confirmed by titration with $BaCl_2$ according to Refs. [43–45]. The CO_2 partial pressure was monitored with the CO_2 sensor on the outlet gas stream.

3. Results and discussion

3.1. Microwave heating and cooling profiles

In order to gauge their response to microwave heating within the current experimental setup, samples of water, 30 wt% MEA and a 30 wt% MEA solution contacted with 20% CO_2 for 20 min

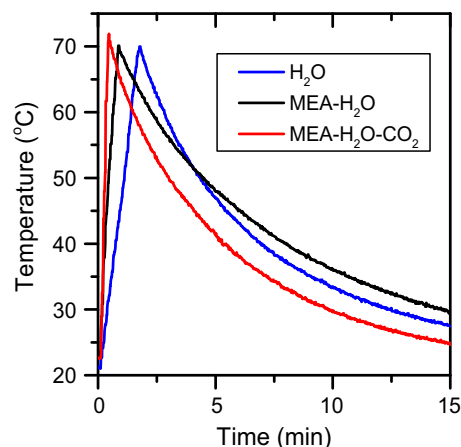


Fig. 2. Microwave heating (100 W) to 70 °C and cooling profiles of the different components of the CO_2 -MEA- H_2O system with 100 mL/min N_2 purge.

were heated in the microwave applicator at 100 W from ambient temperatures to 70 °C and left to cool. Fig. 2 displays the heating and cooling profiles. Each component is observed to heat rapidly followed by cooling back to ambient temperature. The heating rate increases from $H_2O < MEA-H_2O < CO_2$ -MEA- H_2O , where the CO_2 -loaded system heats around five times faster than the pure water system. With all other conditions the same, the rate of microwave heating directly depends on the sample's dielectric loss and heat capacity [24]. The heating rates are consistent with the heat capacities of each component, 4184 J kg⁻¹ K⁻¹ (water), 3734 J kg⁻¹ K⁻¹ (30 wt% MEA) and 3359 J kg⁻¹ K⁻¹ (CO_2 -loaded 30 wt% MEA), respectively [46]. When presented with a mixture of different dielectrics, the microwaves will selectively couple to the higher loss component [38]. The responses of MEA and water solutions to microwave heating are in accordance with recent molecular dynamics simulations [26]. The formation of the carbamate and other ionic species in the CO_2 -loaded solution may generate additional heat via stronger coupling with microwaves compared to the case without absorbed CO_2 . This demonstrates the suitability of the CO_2 -MEA- H_2O system to microwave regeneration.

3.2. Comparison between microwave and conventional regeneration

An aqueous 30 wt% MEA solution was first loaded with CO_2 via an initial absorption step with an inlet gas stream of 20% CO_2 balanced by N_2 (this CO_2 composition is broadly representative of a wide range of large-scale flue gas compositions, from fossil fuelled power plants through to industrial cement works). The CO_2 -rich solution was then regenerated by microwave heating in the pres-

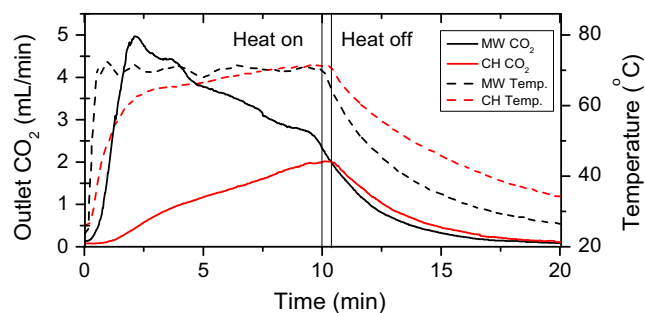


Fig. 3. Comparison of microwave (MW) and conventional heating (CH) to regenerate the CO_2 -loaded MEA solution after an initial absorption step of 20 min with 20% CO_2 .

ence of a purge flow of 100 mL/min N₂ to produce a CO₂-lean solution. The CO₂ desorption profiles and solution temperatures are outlined in Fig. 3. In order to provide a benchmark against conventional heating, the microwave regeneration is compared with that using only a thermal heat source, with the aim to closely reproduce the temperature profile within the sample generated by the microwave experiments. This was achieved by heating in a water bath at 75 °C, followed by removal of the heat bath and maintaining a purge flow of 100 mL/min N₂, the results of which are also shown in Fig. 3. The two temperature profiles in Fig. 3 are quite similar overall, however the microwave heating rate is somewhat faster than the conventional heating rate. This demonstrates the remote and volumetric nature of microwave heating compared to conventional heating, the latter being restricted by conductive heat transfer. Both temperatures reduce quickly under nitrogen purge when heating is stopped, although cooling following microwave heating is somewhat faster. This is again illustrative of the direct interaction of microwaves with the solution without appreciably heating the reactor vessel.

However, despite similar temperature profiles, the CO₂ desorption profiles in Fig. 3 display strikingly different characteristics. During microwave heating CO₂ is rapidly released, peaking at early times (around 4 min) and steadily decreasing as CO₂ is removed until microwave irradiation stops. The thermal heating CO₂ desorption profile on the other hand emerges slowly and with a much smaller peak towards the end of the heating period. Overall, microwave heating releases more than double the amount of CO₂ compared to conventional heating during this single-cycle experiment. The observed differences between conventional and microwave regeneration do *not* appear to reflect the differences between the temperature profiles in Fig. 3, since these are quite close. In particular, the temperature profiles are not very different after two minutes, yet the microwave CO₂ recovery profile peaks at around 4 min, while the thermal CO₂ recovery profile peaks only when thermal heating stops. Clearly, there is a significant microwave effect at play, i.e. the microwave field enhances regeneration beyond that caused by a change in the temperature alone. It therefore appears that a portion of the microwave energy is channelled into reversing the capture reaction without heating the solution.

For microwave regeneration of solid adsorbents, authors frequently refer to ‘inverted thermal temperature gradients’ that arise as a consequence of heat being generated directly inside the adsorbent bed rather than from a stripping medium or the column surface [24,29,37]. The heat transfer direction therefore flows from the inside to the outside of the irradiated material, potentially promoting mass transport and diffusion of the desorbing molecules. Even if this hypothesis were shown to be correct for microwave desorption from a solid adsorbent fixed bed, the continuous mixing of the solution by the bubbling gas in this work will provide a much more isotropic heating profile. Others suggest that changes to the structure and dynamics of the solution due to the microwave field may promote diffusion [42]. However, we consider this unlikely in this case given that CO₂ itself is quadrupolar and therefore largely unaffected by microwaves. The nature of this apparent non-thermal effect might be due to the oscillation of polar functional groups under microwave irradiation to facilitate breaking the bond between CO₂ and amine moieties. This will be investigated next.

3.3. CO₂ absorption isotherms

Many researchers have measured the equilibrium properties of the CO₂-MEA-H₂O system at different thermodynamic conditions, observing a relatively high solubility even at low CO₂ partial pressures [43–45,47–49]. Microwaves selectively couple with components possessing the highest dielectric loss [38]. The possibility that microwaves specifically target the carbamate to provide the

improved CO₂ recovery seen in Fig. 3 should be considered. Inspection of the heating profiles in Fig. 2 lends some support to this possibility. We therefore propose that the non-thermal effects are related to one or more of the following: (i) an increase in the free energy (activity, or chemical potential) of the carbamate state relative to the neutral amine, (ii) a reduction in the activation energy for the reverse capture reaction, or (iii) an increase in the Arrhenius pre-exponential factor for the reverse reaction. Investigation into non-thermal effects and targeted microwave heating of the carbamate can be achieved by measuring CO₂ solubility for absorption isotherms under both conventional heating and microwave irradiation.

Solution CO₂ loadings and outlet gas concentrations were analysed after attainment of steady-state for two different inlet CO₂ partial pressures at a constant temperature of 65 °C using microwave irradiation and thermal heating via a water bath. The first inlet CO₂ partial pressure was 20 kPa, and after reaching steady-state this was increased to 29 kPa. The case of thermal heating corresponds to an equilibrium absorption measurement. The microwave heating case corresponds to a steady-state process, since heat is generated by the microwaves and dissipated to the surroundings. Nevertheless, due to the constant bubbling, we can expect the temperature distribution within the bubbler to be practically uniform and almost identical for the microwave and thermal cases. Any differences between the two heating methods could illuminate non-thermal contributions to the carbamate activity caused by interaction with the microwave field. The resulting isotherms are depicted in Fig. 4.

The two techniques in Fig. 4(a) appear by eye to be very similar. Closer comparison of the CO₂ breakthrough curves for the two data sets suggests that the presence of a microwave field actually permits a slightly higher CO₂ loading relative to conventional heating. The equilibrium CO₂ loadings from the absorption isotherm measurements were confirmed both by comparison to a blank run and by titration of the solution with BaCl₂ and are displayed in Fig. 4(b), which agree quite well with literature data for conventional CO₂-MEA-H₂O solubility measurements [43–45,47–49]. When the inlet partial pressure is increased from 20 kPa to 29 kPa, both techniques follow very similar behaviour with the outlet partial pressures increasing accordingly. If the activity of the carbamate were to increase relative to neutral amine due to interaction with the microwave field, then the reaction equilibrium would shift to favour reactants (compared with true thermal equilibrium at the same temperature), resulting in lower steady-state CO₂ loading and faster breakthrough compared to conventional heating. In fact, microwave irradiation gives a slightly longer breakthrough time and marginally higher solubility. Therefore, it appears that we can rule out a relative increase in the carbamate activity in the presence of microwaves as the cause for the very fast recovery of CO₂ in Fig. 3. We are then left with the possibility that the microwave field reduces the activation energy barrier, or increases the Arrhenius pre-exponential factor, of the reverse capture reaction.

3.4. Multiple microwave regeneration cycles

Due to the continuous and cyclic nature of a conventional MEA stripping process, the aim is to operate at a high working capacity over a narrow loading range. Moreover, desorption should take place quickly to permit fast cycle times, and hence reduce capital costs [7]. A target of 50% CO₂ recovery is often sought (i.e. 50% of the CO₂ content of the rich amine stream is recovered), however industrial systems typically operate at capture efficiencies as low as 15–30% [22]. The feasibility and steady-state performance of the microwave regeneration process was evaluated by completing multiple (six) back-to-back absorption-desorption cycles. The

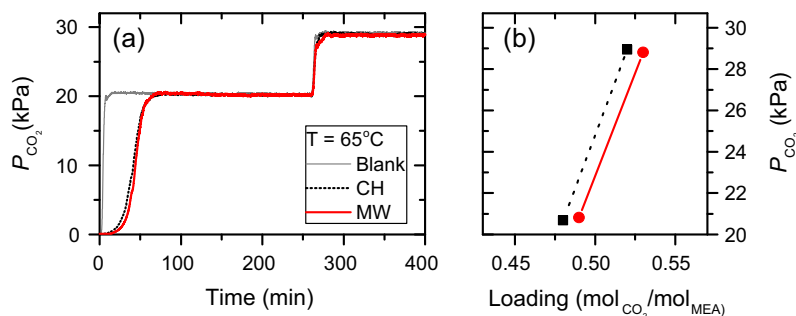


Fig. 4. (a) The CO_2 outlet concentrations versus time for the absorption isotherm measurements at 65°C for microwave (MW) and conventional heating (CH). The initial inlet CO_2 partial pressure of 20 kPa was increased to 29 kPa after sufficient equilibration time. (b) Equilibrium CO_2 loadings and outlet partial pressures from the isotherm measurements.

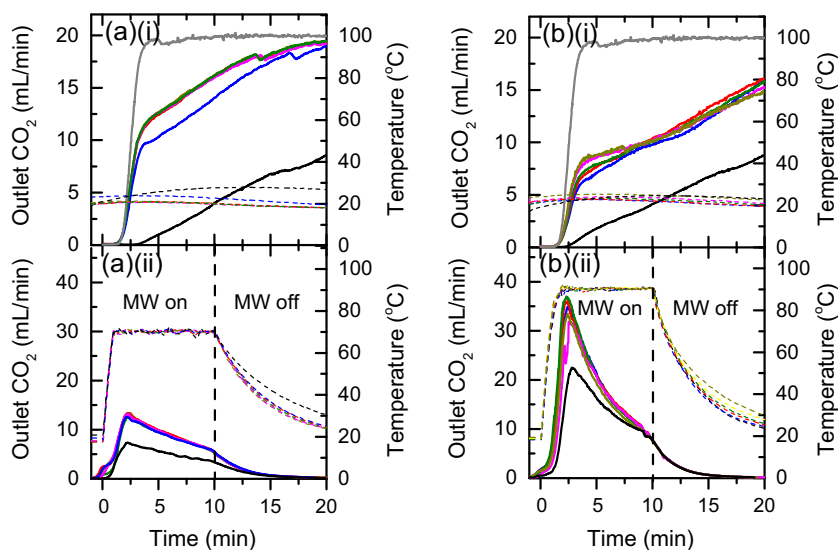


Fig. 5. Breakthrough curves (solid lines) and temperatures (dashed lines) for six back-to-back absorption-desorption cycles using microwave regeneration. (a) Regeneration at 70°C . (b) Regeneration at 90°C . (i) Absorption step. (ii) Desorption step. Cycle number: 1 (black), 2 (blue), 3 (red), 4 (green), 5 (magenta), 6 (dark yellow). (For interpretation of the references to colour in this figure legend, the reader is referred to the web version of this article.)

amine solution was loaded with an inlet gas stream of 20% CO_2 balanced by N_2 without heating. The CO_2 -rich solution was regenerated by microwave irradiation at either 70°C or 90°C to produce a CO_2 -lean solution. The breakthrough curves and solution temperatures of the multiple absorption-desorption cycles are outlined in Fig. 5. A blank run was also performed to allow the absorbed CO_2 quantity to be determined. Apparent in Fig. 5, a large difference between the blank and first absorption runs indicates an initial loading of the solution with CO_2 . A portion of the bound CO_2 is then recovered during the first desorption step. This partial recovery results in a lean solution in which some CO_2 remains. The next absorption step then increases the total loading and subsequent regeneration produces more CO_2 relative to the first desorption step. This is reflected in the outlet CO_2 flow rates in Fig. 5(i). A higher lean loading means less CO_2 is absorbed from the inlet gas stream and so the outlet CO_2 concentration moves towards that of the blank. This trend continues until the solution reaches a steady-state limit, generally between one and two cycles.

As the lean loading increases, the heat of absorption decreases, and so aside from the first step, heat generated during absorption does not vary significantly over consecutive cycles. Rapid microwave heating to the target regeneration temperature occurs, consistent with the direct and volumetric nature of microwave heating. This very fast temperature increase quickly generates an appreciable amount of CO_2 , as seen from the desorption curves,

which peak at early times and decline as more CO_2 is removed. The breakthrough curves suggest an overall stable cyclic working capacity, where regeneration can take place at temperatures considerably lower than the industrial benchmark [5,9]. Comparison of Figs. 5(a) and 5(b) clearly demonstrates an enhanced CO_2 recovery at 90°C compared to 70°C . This is evidenced in both the absorption and desorption curves, where much more CO_2 is released at 90°C , allowing a larger re-uptake in the absorption step to reach steady-state. The CO_2 desorption profile reaches a higher peak at 90°C and declines more rapidly than for 70°C , indicating a faster desorption rate at higher temperature. In the same respect, the absorption profile following 70°C regeneration produces a higher CO_2 outlet concentration sooner than after 90°C regeneration, indicating a lower CO_2 re-uptake due to a higher lean loading.

Integration of the CO_2 curves from Fig. 5, normalized by the number of moles of MEA, permits the rich and lean loadings to be calculated. These are displayed in Fig. 6 for 70°C and 90°C regeneration along with the percentage CO_2 recovery for each cycle. Fig. 6 supports the key findings drawn from Fig. 5. The first absorption-desorption loadings are lower than for subsequent cycles, reflecting the initial loading phase of the system as it approaches steady-state. Both temperature sets display stable cyclic CO_2 capacities over finite loading ranges, with average rich loadings of around $0.5 \text{ mol CO}_2/\text{mol MEA}$, indicating high capture efficiencies over consecutive cycles. Regeneration at 70°C pro-

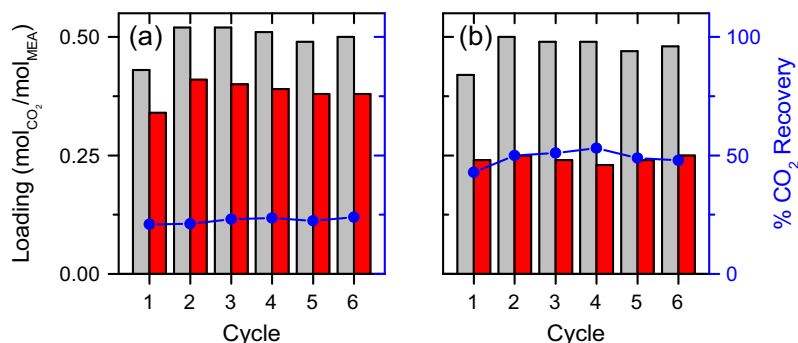


Fig. 6. Rich (grey bars) and lean (red bars) CO₂ loadings for (a) 70 °C regeneration cycles and (b) 90 °C regeneration cycles. The percentage CO₂ recovered between the absorption and desorption steps are shown as blue points. (For interpretation of the references to colour in this figure legend, the reader is referred to the web version of this article.)

duces an average lean loading of 0.39 mol/mol with around 23% CO₂ recovery each time, which lies within the acceptable working range [7]. Regeneration at 90 °C doubles the CO₂ recovery to around 50%, providing lean loadings of 0.25 mol/mol. This is the optimum target for MEA scrubbing and has been achieved at temperatures 30–50 °C lower than with conventional methods [18]. Increasing the regeneration temperature even further could provide a higher percentage CO₂ recovery, however this is not necessary, as optimal cyclic loadings have already been achieved at the lower regeneration temperatures used.

4. Conclusions

Post-combustion CO₂ capture and recovery provides the greatest near-term potential to reduce global CO₂ emissions. In this regard, the feasibility of microwave swing regeneration as an effective alternative to conventional amine scrubbing technology has been investigated for the prototypical 30 wt% MEA system. This amine solution was found to heat rapidly upon microwave irradiation, which is attributed to the favourable dielectric properties of the solutes. Remarkably different CO₂ desorption profiles are obtained when microwave regeneration is compared with conventional thermal heating, with microwave irradiation in our experiments releasing more than double the amount of CO₂ released by conventional heating and at a much faster rate. In order to elucidate the reasons behind this, CO₂ absorption isotherms were performed at 65 °C for both microwave and conventional heating. Comparative isotherms suggest that microwave irradiation also exhibits non-thermal character resulting from reduction of the activation energy, or an increase in the Arrhenius pre-exponential factor, for reversal of the CO₂ capture reaction. Multiple microwave regeneration cycles exhibit consistent and favourable cyclic stability. Average rich loadings of 0.5 mol/mol indicate good capture efficiencies in each absorption step, followed by an average 23% CO₂ recovery for 70 °C regeneration, which is within an acceptable working range, and 50% recovery for 90 °C regeneration, the target industrial recovery rate for MEA scrubbing. To summarize, the high regeneration temperatures (120–140 °C) and slow recovery of conventional MEA scrubbing lead to large energy penalties and solvent losses through evaporation and thermal degradation, in addition to high capital costs [5,9]. The rapid heating, low regeneration temperatures (70–90 °C), fast recovery and cyclic stability in MSR might significantly reduce these problems.

This paper has demonstrated how microwave irradiation can be used as an alternative to conventional heating for recovery of CO₂ from spent MEA solutions at the laboratory scale. Commercial scale-up of microwave heating has already been achieved in other

industries, for example in the processing of metal ore, air drying and VOC recovery, respectively [25]. It should therefore be entirely reasonable for commercial scale microwave regeneration of amine solutions for post-combustion carbon capture to be attained. Furthermore, microwave heating could be utilised alongside low grade industrial heat waste to help reduce capital costs further.

Acknowledgements

The authors gratefully acknowledge funding from the Engineering and Physical Sciences Research Council (EPSRC) under grants EP/N024672/1, EP/J019720/1 and EP/J019704/1. Andrew MacDonald (University of Edinburgh) is thanked for contributions to some of the experimental work.

References

- [1] US Department of Commerce N. ESRL Global Monitoring Division – Global Greenhouse Gas Reference Network n.d. <<http://www.esrl.noaa.gov/gmd/ccgg/trends/>> [accessed December 28, 2015].
- [2] User S. Global Carbon Emissions. CO₂Earth n.d. <<https://www.co2.earth/global-co2-emissions?itemid=1&Fitemid=1>> [accessed April 12, 2016].
- [3] Energy Technology Transitions for Industry: Strategies for the Next Industrial Revolution – industry2009.pdf n.d. <<https://www.iea.org/publications/freepublications/publication/industry2009.pdf>> [accessed December 29, 2015].
- [4] Wang M, Lawal A, Stephenson P, Sidders J, Ramshaw C. Post-combustion CO₂ capture with chemical absorption: a state-of-the-art review. *Chem Eng Res Des* 2011;89:1609–24. <http://dx.doi.org/10.1016/j.cherd.2010.11.005>.
- [5] Boehm RF, Yang H, Yan J, editors. *Handbook of clean energy systems*. Chichester, West Sussex: John Wiley & Sons Inc; 2015.
- [6] Rochelle GT. Carbon Capture and Storage: How Green Can Black Be? *Chem Eng Res Des* 2009;325:1647–52. <http://dx.doi.org/10.1126/science.1172246>.
- [7] Hook RJ. An investigation of some sterically hindered amines as potential carbon dioxide scrubbing compounds. *Ind Eng Chem Res* 1997;36:1779–90.
- [8] Ziaii S, Rochelle GT, Edgar TF. Dynamic modeling to minimize energy use for CO₂ capture in power plants by aqueous monoethanolamine. *Ind Eng Chem Res* 2009;48:6105–11. <http://dx.doi.org/10.1021/ie801385q>.
- [9] Yu C-H. A review of CO₂ capture by absorption and adsorption. *Aerosol Air Qual Res* 2012. <http://dx.doi.org/10.4209/aaqr.2012.05.0132>.
- [10] Dutcher B, Fan M, Russell AG. Amine-based CO₂ capture technology development from the beginning of 2013—A review. *ACS Appl Mater Interfaces* 2015;7:2137–48. <http://dx.doi.org/10.1021/am507465f>.
- [11] Danckwerts PV. The reaction of CO₂ with ethanolamines. *Chem Eng Sci* 1979;34:443–6.
- [12] Crooks JE, Donnellan JP. Kinetics and mechanism of the reaction between carbon dioxide and amines in aqueous solution. *J Chem Soc Perkin Trans* 1989;2:331–3.
- [13] Lv B, Guo B, Zhou Z, Jing G. Mechanisms of CO₂ capture into monoethanolamine solution with different CO₂ loading during the absorption/desorption processes. *Environ Sci Technol* 2015;49:10728–35. <http://dx.doi.org/10.1021/acs.est.5b02356>.
- [14] Faramarzi L, Kontogeorgis GM, Michelsen ML, Thomsen K, Stenby EH. Absorber model for CO₂ capture by monoethanolamine. *Ind Eng Chem Res* 2010;49:3751–9. <http://dx.doi.org/10.1021/ie901671f>.
- [15] Gouedard C, Picq D, Launay F, Carrette P-L. Amine degradation in CO₂ capture. I. A review. *Int J Greenhouse Gas Control* 2012;10:244–70. <http://dx.doi.org/10.1016/j.ijggc.2012.06.015>.

- [16] Lin Y-J, Madan T, Rochelle GT. Regeneration with rich bypass of aqueous piperazine and monoethanolamine for CO₂ capture. *Ind Eng Chem Res* 2014;53:4067–74. <http://dx.doi.org/10.1021/ie403750s>.
- [17] Shakerian F, Kim K-H, Szulejko JE, Park J-W. A comparative review between amines and ammonia as sorptive media for post-combustion CO₂ capture. *Appl Energy* 2015;148:10–22. <http://dx.doi.org/10.1016/j.apenergy.2015.03.026>.
- [18] Ahn H, Luberti M, Liu Z, Brandani S. Process simulation of aqueous MEA plants for post-combustion capture from coal-fired power plants. *Energy Proc* 2013;37:1523–31. <http://dx.doi.org/10.1016/j.egypro.2013.06.028>.
- [19] Dugas RE, Rochelle GT. CO₂ absorption rate into concentrated aqueous monoethanolamine and piperazine. *J Chem Eng Data* 2011;56:2187–95. <http://dx.doi.org/10.1021/jie101234t>.
- [20] Webley PA, Zhang J. Microwave assisted vacuum regeneration for CO₂ capture from wet flue gas. *Adsorption* 2014;20:201–10. <http://dx.doi.org/10.1007/s10450-013-9563-y>.
- [21] Chronopoulos T, Fernandez-Diez Y, Maroto-Valer MM, Ocone R, Reay DA. CO₂ desorption via microwave heating for post-combustion carbon capture. *Microporous Mesoporous Mater* 2014;197:288–90. <http://dx.doi.org/10.1016/j.micromeso.2014.06.032>.
- [22] Yang J, Tan HY, Low QX, Binks BP, Chin JM. CO₂ capture by dry alkanolamines and an efficient microwave regeneration process. *J Mater Chem A* 2015;3:6440–6. <http://dx.doi.org/10.1039/C4TA06273F>.
- [23] Nigar H, Garcia-Baños B, Peñaranda-Foix FL, Catalá-Civera JM, Mallada R, Santamaría J. Amine-functionalized mesoporous silica: a material capable of CO₂ adsorption and fast regeneration by microwave heating. *AIChE J* 2016;62:547–55. <http://dx.doi.org/10.1002/aic.15118>.
- [24] Cherbański R, Molga E. Intensification of desorption processes by use of microwaves—An overview of possible applications and industrial perspectives. *Chem Eng Process Process Intensif* 2009;48:48–58. <http://dx.doi.org/10.1016/j.ccep.2008.01.004>.
- [25] Bathen D. Physical waves in adsorption technology—An overview. *Sep Purif Technol* 2003;33:163–77. [http://dx.doi.org/10.1016/S1383-5866\(03\)00004-2](http://dx.doi.org/10.1016/S1383-5866(03)00004-2).
- [26] Cardona J, Fartaria R, Sweatman MB, Lue L. Molecular dynamics simulations for the prediction of the dielectric spectra of alcohols, glycols and monoethanolamine. *Mol Simul* 2016;42:370–90. <http://dx.doi.org/10.1080/08927022.2015.1055741>.
- [27] Mingos DMP, Baghurst DR. Tilden Lecture. Applications of microwave dielectric heating effects to synthetic problems in chemistry. *Chem Soc Rev* 1991;20:1–47.
- [28] Meredith RJ. *Engineers' handbook of industrial microwave heating*. IET; 1998.
- [29] Cherbański R, Komorowska-Durka M, Stefanidis GD, Stankiewicz AI. Microwave swing regeneration vs temperature swing regeneration—comparison of desorption kinetics. *Ind Eng Chem Res* 2011;50:8632–44. <http://dx.doi.org/10.1021/ie102490v>.
- [30] Hashisho Z, Emamipour H, Cevallos D, Rood MJ, Hay KJ, Kim BJ. Rapid response concentration-controlled desorption of activated carbon to dampen concentration fluctuations. *Environ Sci Technol* 2007;41:1753–8. <http://dx.doi.org/10.1021/es062155v>.
- [31] Hashisho Z, Emamipour H, Rood MJ, Hay KJ, Kim BJ, Thurston D. Concomitant adsorption and desorption of organic vapor in dry and humid air streams using microwave and direct electrothermal swing adsorption. *Environ Sci Technol* 2008;42:9317–22. <http://dx.doi.org/10.1021/es801285v>.
- [32] Chowdhury T, Shi M, Hashisho Z, Kuznicki SM. Indirect and direct microwave regeneration of Na-ETS-10. *Chem Eng Sci* 2013;95:27–32. <http://dx.doi.org/10.1016/j.ces.2013.02.061>.
- [33] Chowdhury T, Shi M, Hashisho Z, Sawada JA, Kuznicki SM. Regeneration of Na-ETS-10 using microwave and conductive heating. *Chem Eng Sci* 2012;75:282–8. <http://dx.doi.org/10.1016/j.ces.2012.03.039>.
- [34] Fayaz M, Shariaty P, Atkinson JD, Hashisho Z, Phillips JH, Anderson JE, et al. Using microwave heating to improve the desorption efficiency of high molecular weight VOC from beaded activated carbon. *Environ Sci Technol* 2015;49:4536–42. <http://dx.doi.org/10.1021/es505953c>.
- [35] Mao H, Zhou D, Hashisho Z, Wang S, Chen H, (Helena) Wang H. Constant power and constant temperature microwave regeneration of toluene and acetone loaded on microporous activated carbon from agricultural residue. *J Ind Eng Chem* 2015;21:516–25. <http://dx.doi.org/10.1016/j.jiec.2014.03.01>.
- [36] Shi M, Lin CCH, Kuznicki TM, Hashisho Z, Kuznicki SM. Separation of a binary mixture of ethylene and ethane by adsorption on Na-ETS-10. *Chem Eng Sci* 2010;65:3494–8. <http://dx.doi.org/10.1016/j.ces.2010.02.048>.
- [37] Ania CO, Parra JB, Menéndez JA, Pis JJ. Effect of microwave and conventional regeneration on the microporous and mesoporous network and on the adsorptive capacity of activated carbons. *Microporous Mesoporous Mater* 2005;85:7–15. <http://dx.doi.org/10.1016/j.micromeso.2005.06.013>.
- [38] Polært I, Ledoux A, Estel L, Huyghe R, Thomas M. Microwave assisted regeneration of zeolite. *Int J Chem React Eng* 2007;5.
- [39] Polært I, Estel L, Huyghe R, Thomas M. Adsorbents regeneration under microwave irradiation for dehydration and volatile organic compounds gas treatment. *Chem Eng J* 2010;162:941–8. <http://dx.doi.org/10.1016/j.cej.2010.06.047>.
- [40] Turner MD, Laurence RL, Conner WC, Yngvesson KS. Microwave radiation's influence on sorption and competitive sorption in zeolites. *AIChE J* 2000;46:758–68.
- [41] Vallee SJ, Conner WC. Microwaves and sorption on oxides: a surface temperature investigation. *J Phys Chem B* 2006;110:15459–70. <http://dx.doi.org/10.1021/jp061679h>.
- [42] Antonio C, Deam RT. Can “microwave effects” be explained by enhanced diffusion? *Phys Chem Chem Phys* 2007;9:2976. <http://dx.doi.org/10.1039/b617358f>.
- [43] Jou F-Y, Mather AE, Otto FD. The solubility of CO₂ in a 30 mass percent monoethanolamine solution. *Can J Chem Eng* 1995;73:140–7. <http://dx.doi.org/10.1002/cjce.5450730116>.
- [44] Ma'mun S, Nilsen R, Svendsen HF, Juliussen O. Solubility of carbon dioxide in 30 mass % monoethanolamine and 50 mass % methyldiethanolamine solutions. *J Chem Eng Data* 2005;50:630–4. <http://dx.doi.org/10.1021/je049649>.
- [45] Shen KP, Li MH. Solubility of carbon dioxide in aqueous mixtures of monoethanolamine with methyldiethanolamine. *J Chem Eng Data* 1992;37:96–100.
- [46] Weiland RH, Dingman JC, Cronin DB. Heat capacity of aqueous monoethanolamine, diethanolamine, N-methyldiethanolamine, and N-methyldiethanolamine-based blends with carbon dioxide. *J Chem Eng Data* 1997;42:1004–6.
- [47] Versteeg GF, Van Swaaij W. Solubility and diffusivity of acid gases (carbon dioxide, nitrous oxide) in aqueous alkanolamine solutions. *J Chem Eng Data* 1988;33:29–34.
- [48] Cheng M-D, Caparanga AR, Soriano AN, Li M-H. Solubility of CO₂ in the solvent system (water+monoethanolamine+triethanolamine). *J Chem Thermodyn* 2010;42:342–7. <http://dx.doi.org/10.1016/j.jct.2009.09.005>.
- [49] Aronu UE, Gondal S, Hessen ET, Haug-Warberg T, Hartono A, Hoff KA, et al. Solubility of CO₂ in 15, 30, 45 and 60 mass% MEA from 40 to 120 °C and model representation using the extended UNIQUAC framework. *Chem Eng Sci* 2011;66:6393–406. <http://dx.doi.org/10.1016/j.ces.2011.08.042>.